Journal of Hazardous Materials 275 (2014) 63–71

Contents lists available at ScienceDirect

Journal of Hazardous Materials

journal homepage: www.elsevier.com/locate/jhazmat

Application of cetyltrimethylammonium bromide bentonite–titanium dioxide photocatalysis technology for pretreatment of aging leachate

Fei-Fei Cai[a], Zhao-Hui Yang[a,*], Jing Huang[a], Guang-Ming Zeng[a], Li-ke Wang[a], Jian Yang[b]

[a] *College of Environmental Science and Engineering, Hunan University, Changsha 410082, China*
[b] *The Quality Supervision and Management Station of Civil Air Defense Engineering of Changsha City, China*

HIGHLIGHTS

- An innovative approach of combining organobentonite and TiO_2 was applied to pretreat aging leachate.
- Composite organobentonite was characterized by FESEM/EDS and FTIRS.
- Removing of COD and NH_3-N relied on both adsorption and photocatalysis.
- Removal efficiency of simultaneous utilizing CTMAB2.5 and TiO_2 was better than them in succession.
- The technology showed superior removal rates of COD and NH_3-N, up to 89% and 61%, respectively.

ARTICLE INFO

Article history:
Received 21 October 2013
Received in revised form 18 March 2014
Accepted 22 April 2014
Available online 29 April 2014

Keywords:
Leachate
Organobentonite
Adsorption
TiO_2
Photocatalysis

ABSTRACT

Organobentonite–photocatalysis technology was applied to pretreat aging leachate containing refractory pollutants. The organobentonite was synthesized by organic modifier cetyltrimethylammonium bromide (CTMAB) and natural bentonite. In characterization experiments, we could confirm that organic functional groups of cetyltrimethylammonium ($CTMA^+$) cations were successfully loaded on the surface of bentonite. The combination of CTMAB2.5 adsorption and TiO_2 photocatalysis was superior to either running separately. Furthermore, removal efficiency of simultaneously utilizing CTMAB2.5 and TiO_2 was better than them in succession. The combination technology was feasible and was optimized by response surface methodology (RSM) with COD and NH_3-N removal rate as the target responses. The optimal operation conditions calculated from the regression equations were CTMAB2.5 dosage of 7.5 g/L, pH at 3.5, TiO_2 dosage of 1.63 g/L, and reaction time for 60.02 min, which maintained the removal of COD and NH_3-N at 82% and 37%, respectively.

1. Introduction

While sanitary landfill is regarded as an economical and environmental method to deal with solid wastes, the leachate containing many toxic contaminates from the landfills has great threat to groundwater and surrounding soil [1]. The leachate mainly derives from percolating rainwater, containing water of the wastes piles and the degradation of organic fraction [2]. Thus, characteristics of leachate predominantly depend on ingredients of solid garbage and the biological and chemical reaction processing in the landfill as well as the climate, hydrogeology, ages and landfill size [3–5]. In addition, the leachate has complex ingredients with high concentrations of organic compounds and ammonia, at the top strengths of 5000–20,000 mg/L and 3000–5000 mg/L, respectively [3,4]. If the leachate is not treated appropriately and discharged directly into groundwater, it will cause serious consequences such as hypoxia, eutrophication and deterioration of the water [2–4].

In recent years, biological techniques, with advantages of reliability, simplicity and low cost, can show reasonable performance when treating young leachate (landfill age <5 years). However, when treating aging leachate (landfill age ≥5 years), physico-chemical treatments can effectively remove refractory substances while biological techniques are not able to do this [6]. Furthermore, physico-chemical treatments are regarded as refining step after biological techniques due to stable quality of discharged water [7]. Additionally, advanced oxidation processes have been researched and applied widely during recent decades because of the ability

---

* Corresponding author. Tel.: +86 0731 88822829; fax: +86 0731 88821413.
E-mail address: yzh@hnu.edu.cn (Z.-H. Yang).

http://dx.doi.org/10.1016/j.jhazmat.2014.04.050
0304-3894/

of decomposing recalcitrant compounds in leachate [2,7]. Because of complex composition and characteristic of the leachate, individual treatment cannot meet environmental requirement and the combination of two or three treatments is more and more applied [8–11].

Adsorption as a kind of physico-chemical treatments is utilized widely. And the bentonite with special features can be regarded as adsorbent. Bentonite is mainly composed of montmorillonite whose structure is one aluminum oxide octahedral sheet in the center of two silicon–oxygen tetrahedral sheets [12]. The isomorphous substitutions of Al^{3+} for Si^{4+} in the tetrahedral sheet and Mg^{2+} or Zn^{2+} for Al^{3+} in the octahedral sheet can cause net negative charges on the surfaces [13]. Unbalance charges are offset by exchanged cations adsorbed on layer surfaces. However, those exchanged cations easily hydrate to form a thin water film. Adsorption of nonionic organic matters from effluent to bentonite is relatively weak due to preferential attraction of polar water molecules to polar mineral surface [14,15]. Moreover, low organic carbon content of bentonite limits nonionic organic compounds sorption by partition into bentonite [14].

Organobentonite is synthesized by natural bentonite and organic modifier. Organic cations are intercalated into the lattice structure of bentonite [16]. In comparison with bentonite, organobentonites have more surface active sited available for adsorption due to the surfaces of transition from hydrophilic to hydrophobic and sorptive phase formed [17–20]. The sorption of organobentonite is mainly influenced by the configuration and loading of organic modifier [12,18–20]. Zhu et al. [12] demonstrated that organobentonites with long alkyl chains of cation surfactants possessed higher removal relative to those with short alkyl chains. Ling et al. [20] treated leachate after pretreatment by struvite with organobentonite modified by dioctadecyl dimethyl ammonium chloride and COD removal was 90%.

Photocatalysis may be termed as photoinduced reaction accelerated by the presence of catalyst [21]. After semiconductor oxides are exposed in photon irradiation, charge separations are formed because of electrons from valence band promoting to conduction band [21–23]. Hence, holes are generated in valence band and electron–hole pairs are produced. Photocatalytic reaction mainly depends on the oxidation of holes. The holes can directly oxidize organic matters, or indirectly oxidize OH^- and H_2O on the surface of catalysts to form hydroxyl radicals ($OH^\bullet$). $OH^\bullet$ can powerfully oxidize organic matters [21–24]. TiO_2, a wide band-gap (3.2 eV) semiconductor, corresponds to radiation in the near-UV range [21,24]. Compared to immobilized TiO_2, suspended TiO_2 can obtain better efficiency because TiO_2 in the state of suspension can freely contact with UV irradiation [25]. Meeroff et al. [25] and Poblete et al. [22] treated the leachate with TiO_2 photocatalysis and the optimal COD removal were up to 71% and 57%, respectively.

Obviously, the leachate treatment by organobentonite adsorption alone and TiO_2 photocatalysis alone was researched but the performance was not superior to combination efficiency. Kurniawan et al. [8] verified that analogous combination of GAC adsorption and ozone oxidation had higher removal efficiency of 86% COD and 92% NH_3-N compared to ozonation alone with 35% COD and 50% NH_3-N.

The main objectives of this paper were two aspects. First, we needed to develop a kind of organobentonite with greater adsorption than natural bentonite. The second goal was to investigate the possibility of pretreating aging leachate with combining organobentonite and photocatalysis and to find optimal operation by response surface methodology. Currently, there is relatively little published information on dealing with aging leachate by organobentonite–photocatalysis technology.

Table 1
Properties of raw leachate.

Constituent	Range	Average	Units
COD	6400–7800	7000	mg/L
BOD_5	685–810	750	mg/L
Ammonia	1660–1770	1700	mg/L
SS	79–94	87	mg/L
Color	300–400	350	PCU
pH	7.8–8.3	8.1	

2. Materials and methods

2.1. Materials

Natural bentonite was chemical grade and from Sihaowei Chemical Co., Ltd., Shanghai. TiO_2 and CTMAB were analytical grade and supplied by Damao Chemical Reagent Factory, Tianjin.

The used leachate was taken from Heimifeng Landfill located in Changsha, China. This plant covers about 174 ha surface, which has been in operation since 2003, and treats more than 3000 tons solid waste daily. The properties of leachate were shown in Table 1.

2.2. Preparation of CTMAB-bentonite

In this study, CTMAB was chosen as organic modifier. $CTMA^+$ can create an organic partition medium through the conglomeration of their flexible and long alkyl chains [12,15].

CTMAB-bentonite was prepared as follows. First, 20 ml HCl and 30 ml H_2SO_4 were added into 750 ml distilled water. Then 100 g natural bentonite was added into the mixture liquor. Thirdly, mixture solution was stirred by magnetic stirrer (ZNCL-S) at the speed of 700 r/min for 3 h at room temperature. Fourthly, 0.6 g polyaluminium chloride (PAC), 0.05 g polyacrylamide (PAM), which were conductive to agglomerate and conglutinate organic modifier and bentonite, and a little CTMAB were added into suspension obtained from the third step. The solution was stirred by magnetic stirrer at the speed of 700 r/min for 5 h at 60 °C. After that, the solution was filtered by stainless steel pressure filter (SHXB-Z-2L). The precipitate was washed until that no silver bromide in the filtrate was generated detected by $AgNO_3$. The precipitate was put in the oven (101A-2) to dry for 4 h at 90 °C and activate for 1 h at 110 °C. Eventually, dried material was grinded into fine power and CTMAB-bentonite was obtained. Optimal additive CTMAB dosage was determined by actual experiments operated under the same condition of 60 min reaction time, 1.5 g/L CTMAB-bentonite dosage and without pH adjustment.

2.3. Characterization of organobentonite

Organobentonite was characterized by Environmental scanning electron microscope (ESEM)/Energy dispersive spectrometer (EDS) (Quanta 200 FEG, FEI, US) and Fourier transform-infrared spectrometer (FTIRS) (FTIR-8400S, IRprestige-21). ESEM was in low vacuum mode at an acceleration potential of 20 kV. Moreover, microanalysis of CTMAB2.5 was carried out with EDS equipped on the Quanta 200. The samples were blended with dry KBr in the agate mortar and were finely powdered to press the KBr pellets. The FTIR spectra in the range of 4000–400 cm^{-1} were reduced at an optical resolution of 2 cm^{-1}.

BET surface area and organic carbon content were measured by specific surface area and pore volume adsorption analyzer (OMNISORP100CX, Coulter, USA) and total organic carbon analyzer (TOC-V CPH, Shimadzu). Particle size and zeta potential was determined by Zetasizer (Nano-ZS90, Malvern, England).

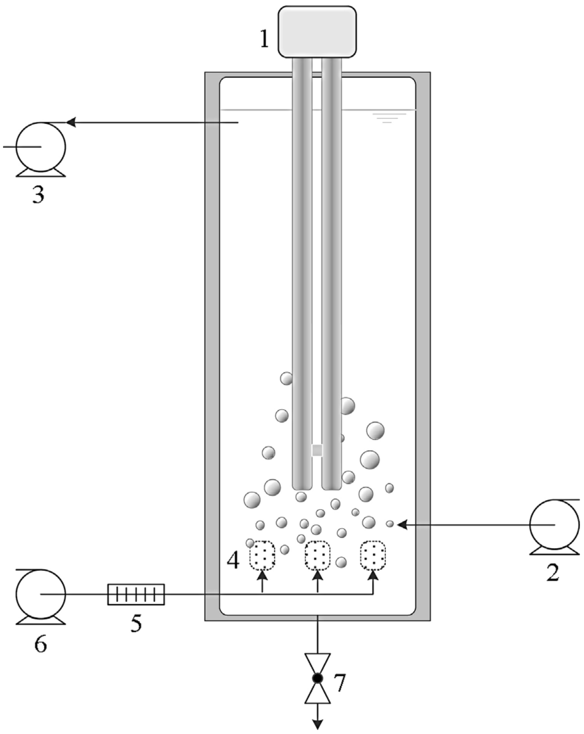

Fig. 1. Schematic diagram of the reactor apparatus used in this study (1: UVC lamp, 2: influent pump, 3: effluent pump, 4: aeration device, 5: rotor flowmeter, 6: air pump, 7: mud valve).

2.4. Procedures for leachate treatment

Fig. 1 displayed the apparatus. Effective volume of reactor (13 cm ID × 20 cm tall) was 2 L. A cylindrical ultraviolet lamp (Xuelaite, ZW18D17Y, 18 W) with two tubes of 21.7 cm length and 1.7 cm diameter was set in the middle of the reactor. The intensity of UV light furnished with 365 nm light was 57 $\mu W/cm^2$ within the range of 100 cm. A micro-aeration head was set at the bottom of reactor. The aeration was maintained at 0.4 L/min. Reactions were conducted at room temperature. Start point of the reaction was treated as the time when organobentonite and TiO_2 were added into leachate adjusted to various pH (pH meter, PB-10) by NaOH and H_2SO_4 and valves of UV lamp and micro-aeration head were opened simultaneously.

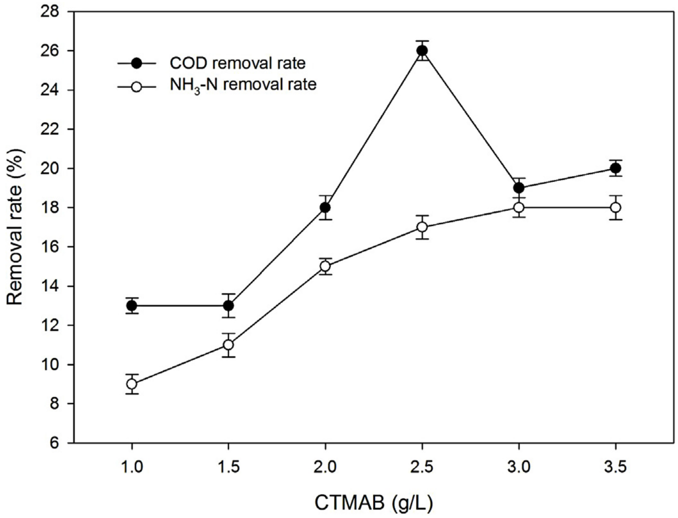

Fig. 2. The effect of CTMAB dosage adding into natural bentonite on COD and NH_3-N removal rate.

2.5. RSM experimental design

Central composite design (CCD), a response surface methodology (RSM), was applied to evaluate the relationship between two responses and four variables, as well as to select optimal conditions of variables and predict the best value of responses. In the design, two responses were removal of COD and NH_3-N, while four variables were organobentonite dosage (x_1), pH (x_2), TiO_2 dosage (x_3) and reaction time (x_4), respectively. All factors were controlled at five levels and the CCD was selected to frame 30 experiments. The response variable (y) was fitted by a second-order polynomial model and expressed in the form of following quadratic Eq. (1):

$$y = \beta_0 + \sum_{i=1}^{m} \beta_i x_i + \sum_{i<j}^{m} \beta_{ij} x_i x_j + \sum_{i=1}^{m} \beta_{ii} {x_i}^2 \qquad (1)$$

where y is the response variable, x_i and x_j are independent variables which confirm y, β_0, β_i and β_{ii} are the offset term, i is the liner coefficient and j is the quadratic coefficient, respectively. β_{ij} is the term that reflects the interaction between x_i and x_j [26,27]. The practical design operated by the statistic software, Design-expert 7.1.3 (Stat-Ease Inc., USA), was displayed in Table 2.

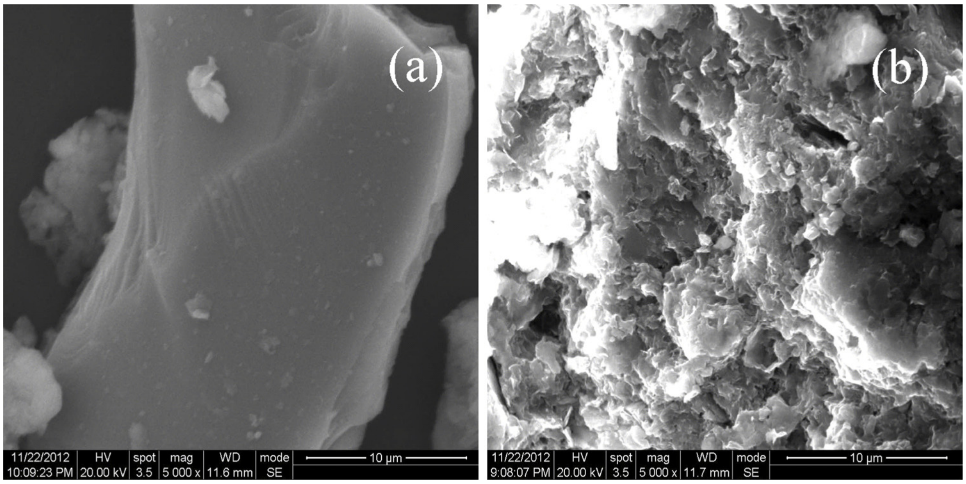

Fig. 3. Environmental scanning electron microscope graphs: (a) SE mode of natural bentonite at 5000×, (b) SE mode of CTMAB2.5 at 5000×.

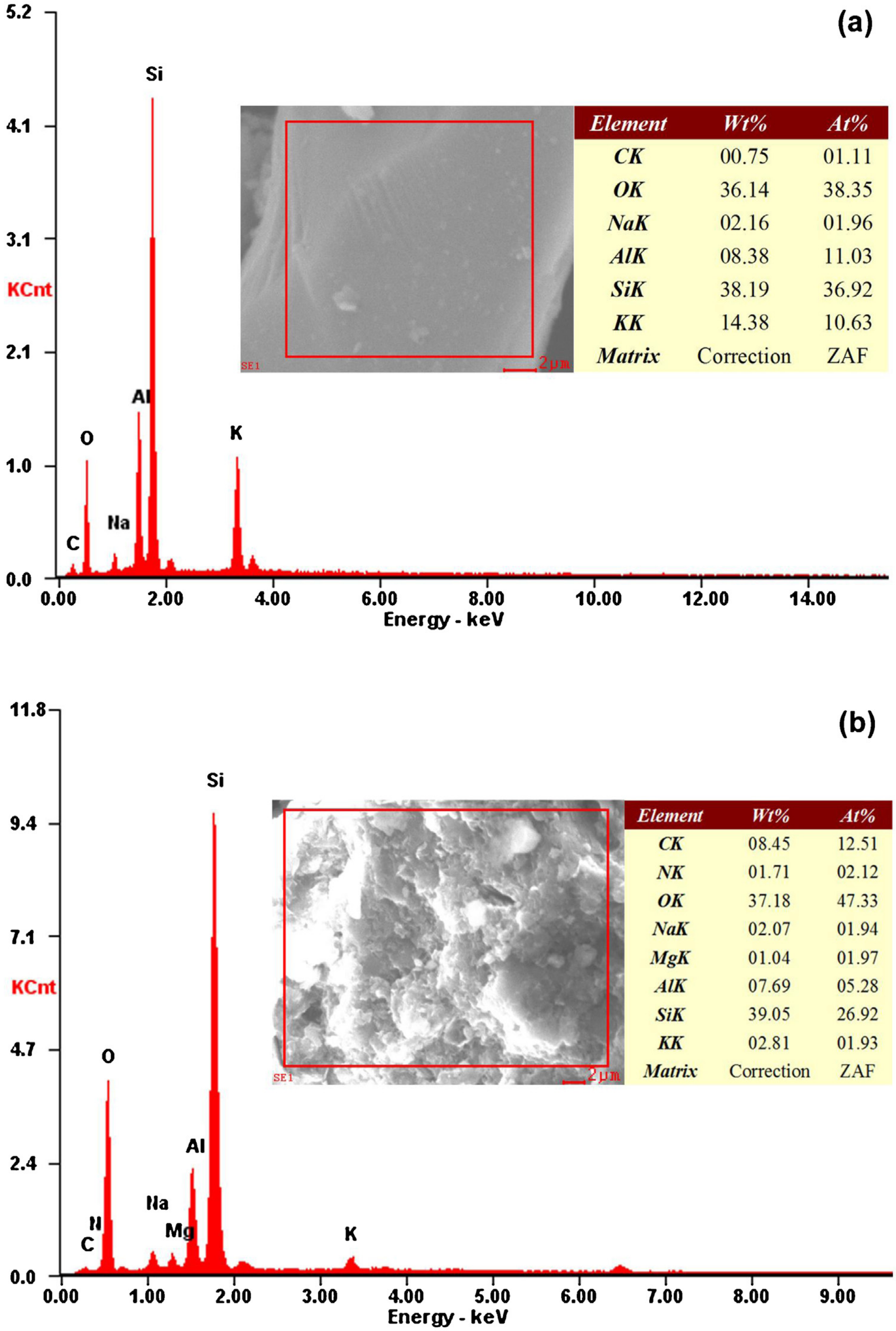

(a)

Element	*Wt%*	*At%*
CK	00.75	01.11
OK	36.14	38.35
NaK	02.16	01.96
AlK	08.38	11.03
SiK	38.19	36.92
KK	14.38	10.63
Matrix	Correction	ZAF

(b)

Element	*Wt%*	*At%*
CK	08.45	12.51
NK	01.71	02.12
OK	37.18	47.33
NaK	02.07	01.94
MgK	01.04	01.97
AlK	07.69	05.28
SiK	39.05	26.92
KK	02.81	01.93
Matrix	Correction	ZAF

Fig. 4. Energy dispersive spectrometer analysis graphs: (a) natural bentonite, (b) CTMAB2.5.

Table 2
Coded levels for 4 variables framed by central composite design (CCD).

Factors	Codes	Coded levels				
		−2.38	−1	0	1	2.38
CTMAB2.5 (g/L)	x_1	0	2.50	5.00	7.50	10.00
pH	x_2	2.00	3.50	5.00	6.50	8.00
TiO_2 (g/L)	x_3	0.50	1.63	2.75	3.88	5.00
Time (min)	x_4	30	60	90	120	150

2.6. Determination methods of two responses

The concentrations of COD and NH_3-N were analyzed according to the environmental protection standards [28,29]. The removal of COD and NH_3-N were gained through the following Eq. (2):

$$\text{Removal rate} = \frac{C_i - C_f}{C_i} \times 100\% \qquad (2)$$

where C_i was initial concentration, C_f was final concentration.

2.7. Statistical analysis

To ensure the accuracy, reliability and reproducibility of the collected data, experiments were carried out at least in triplicate, and the mean value of three data sets is presented. The data except from RSM experiment exceeding relative error 1.0% would be excluded and a fourth experiment would be conducted until the error fell within acceptable range. Statistical tests were performed by SPSS 13.0 windows version with a confidence interval (CI) of 95%. Differences were considered statistically significant when $p \leq 0.05$.

3. Results and discussion

3.1. The analysis of optimal CTMAB dosage

The results were shown in Fig. 2. Obviously, COD and NH_3-N removal firstly ascended with increasing CTMAB dosage, after reaching a peak, COD removal slightly declined while NH_3-N removal tended to be smooth with further CTMAB dosage. With adding CTMAB dosage, the number of quaternary ammonium cation incorporating into bentonite was increasing, which contributed to enhance COD and NH_3-N removal. When there were no more micropores for excess $CTMA^+$ to occupy, superabundant dosage would impact the pollutant removal. According to Fig. 2, the efficiency became better with optimal CTMAB dosage of 2.5 g. So organobentonite was called CTMAB2.5.

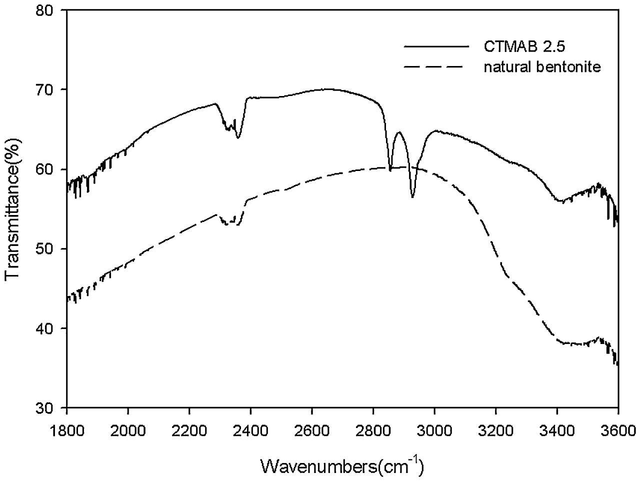

Fig. 5. Fourier transform-infrared spectra of natural bentonite and CTMAB2.5.

Testing of treating leachate with used CTMAB2.5 under the same condition showed similar COD removal performance after multiple. Reused times were more than twice. So the result indirectly revealed that the level of CTMAB released from organobentonite was limited and CTMAB2.5 has the value of repeated use.

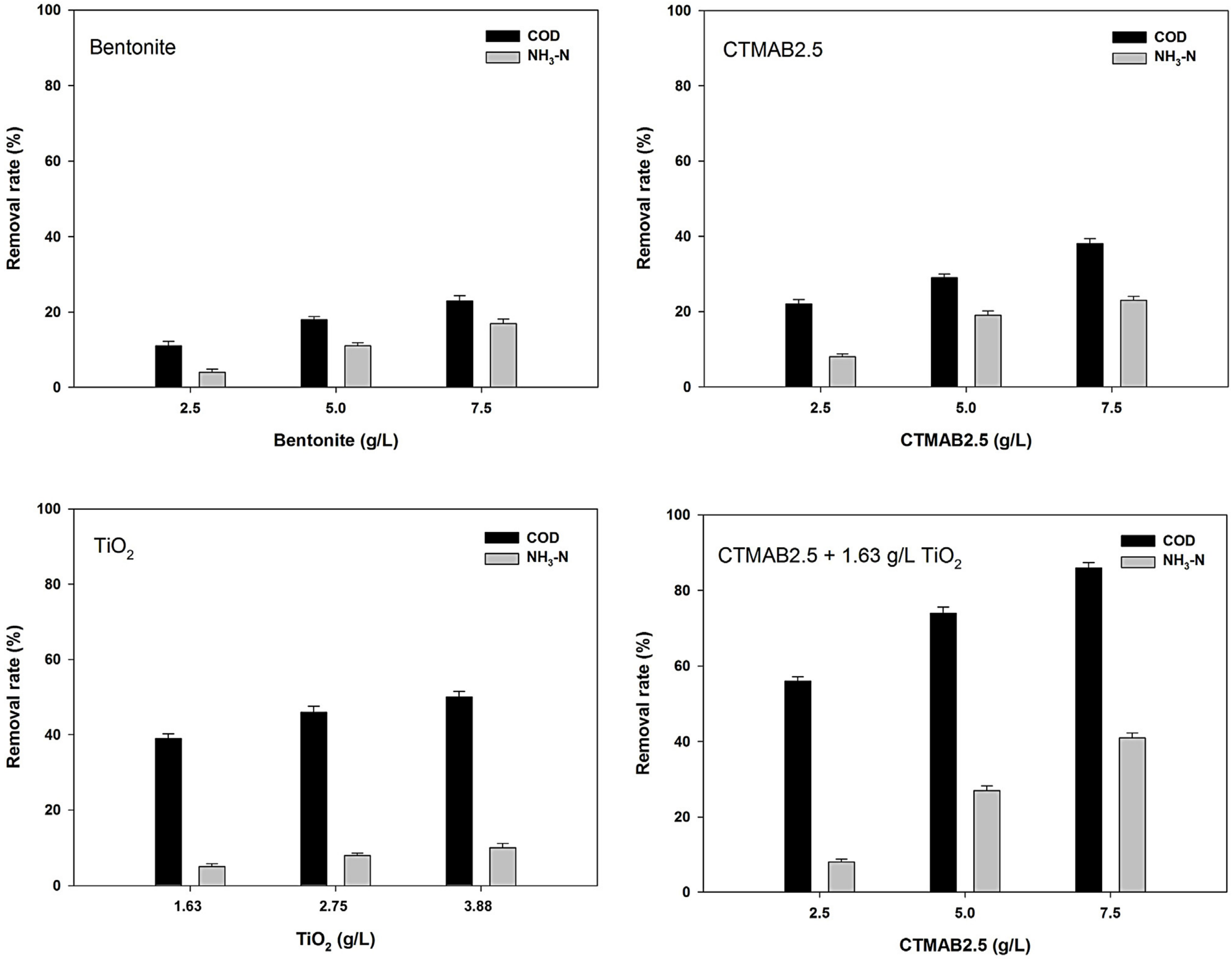

Fig. 6. The different removal rates of COD and NH_3-N among four groups of experiments with reaction time for 60 min and pH at 3.5.

Table 3
CCD design and response values.

Run	Code values				Real values				Response	
	x_1	x_2	x_3	x_4	x_1 (g/L)	x_2	x_3 (g/L)	x_4 (min)	CODRemoval rate (%)	NH_3-NRemoval rate (%)
1	0	2	0	0	5.00	8.00	2.75	90.00	53	24
2	−1	−1	1	−1	2.50	3.50	3.88	60.00	31	10
3	−1	1	1	1	2.50	6.50	3.88	120.00	66	53
...	...	...	...	...	...	...	...	...	...	...
7	0	0	−2	0	5.00	5.00	0.50	90.00	89	17
...	...	...	...	...	...	...	...	...	...	...
10	−1	1	1	−1	2.50	6.50	3.88	60.00	64	61
11	−1	1	1	1	2.50	6.50	3.88	120.00	66	53
...	...	...	...	...	...	...	...	...	...	...
13	1	−1	−1	−1	7.50	3.50	1.63	60.00	76	40
...	...	...	...	...	...	...	...	...	...	...
15	1	−1	−1	1	7.50	3.50	1.63	120.00	72	48
...	...	...	...	...	...	...	...	...	...	...
18	1	1	1	1	7.50	6.50	3.88	120.00	42	43
...	...	...	...	...	...	...	...	...	...	...
28	−1	1	−1	1	2.50	6.50	1.63	60.00	49	16
29	0	0	0	0	5.00	5.00	2.75	90.00	50	16
30	−1	−1	−1	−1	2.50	3.50	1.63	60.00	56	8

3.2. Characterization analysis of CTMAB2.5

In Fig. 3, natural bentonite surface was smooth while CTMAB2.5 surface was rugged and covered with flocs. Furthermore, EDS analysis provided the elementary contents and the results were shown in Fig. 4.

Obvious difference displayed in Fig. 5 between natural bentonite and CTMAB2.5 was two intense bands. Adsorption bands of CTMAB around at 2920 cm^{-1} and 2850 cm^{-1} correspond to CH_2 asymmetric stretch modes and CH_3 symmetric stretch modes, respectively [30,31]. Thus $CTMA^+$ were successfully loaded on natural bentonite surface.

BET surface area, porosity, particle size, the point of zero charge and zeta potential of CTMAB2.5 were 122 m^2/g, 71%, 1560 nm, 2.14 and 5.4 mV, respectively. And these characterizations of natural bentonite were 119 m^2/g, 59%, 1350 nm, 2.11 and −11.3 mV, respectively. Among above data, obvious difference was porosity. The porosity of CTMAB2.5 was higher and the result could infer that the adsorption of CTMAB2.5 was better. The change of zeta potential from the negative of natural bentonite to the positive of CTMAB2.5 implied that $CTMAB^+$ loaded on natural bentonite surface could neutralize negative charges and cause positive charges. Zhu et al. [14] implied that better removal efficiency of organic compounds was closely related to higher content of organic carbon adsorbed into organobentonite. The organic carbon content of CTMAB2.5 was 8.3%, much higher than the organic carbon content of natural bentonite, nearly equal to 0%.

3.3. The combination of CTMAB2.5 adsorption and TiO_2 photocatalysis

Fig. 6 showed that combination of CTMAB2.5 adsorption and TiO_2 photocatalysis was clearly superior to others. The reaction scheme was shown in Fig. 7. And in combination of 7.5 g/L CTMAB2.5 and 1.63 g/L TiO_2, optimal removal efficiencies of COD and NH_3-N were up to 86% and 41%. In comparison with natural bentonite, the performance of CTMAB2.5 was enhanced mainly due to the surfaces transition to hydrophobic and additionally a $CTMA^+$-derived sorptive phase formed [19]. TiO_2 photocatalysis alone showed low NH_3-N removal due to acidic pH and weak intensity of UV light [23]. The fourth group performed best mainly because the combination offered synergistic effects on degradation of refractory pollutants.

Additionally, to compare with the effect of simultaneous combination, CTMAB2.5 adsorption and TiO_2 photocatalysis were divided into two successive steps with pH at 3.5 and time for 60 min. The first step used 7.5 g/L CTMAB2.5 alone. COD declined to 4342 mg/L with 38% removal and NH_3-N reduced to 1311 mg/L with 23% removal ($p \leq 0.05$, paired *t*-test). The second one was to put the supernatant from the first step into another reactor and then add 1.63 g/L TiO_2 with UV lamp on. Finally, COD declined to 2607 mg/L with 40% removal and NH_3-N reduced to 1165 mg/L with 11% removal ($p \leq 0.05$, paired *t*-test). Otherwise, we did another test which reversed the order of two steps and the data showed final results were similar, without significant difference. In comparison with the data of simultaneously integrated CTMAB2.5 and TiO_2 with removal of 86% COD and 41% NH_3-N, removal efficiency of successive experiments was inferior. Likely, CTMAB2.5 might be considered as attractive substrate for TiO_2 catalyst due to its special structure, which effectively promote the dispersion of TiO_2 and provide easy access for contaminants to the photocatalyst. The positive role of SiC on the enhancement of the photocatalysis had been reported [32]. Relevantly deeper theory should be further researched.

Theoretically, aeration was related to the disappearance of COD and NH_3-N. But in fact, with the advance of aeration from 0.4 to 1.2 L/min, COD removal nearly appeared invariability and NH_3-N removal improved no more than 1.5% ($p \leq 0.05$, paired *t*-test) at the condition of 7.5 g/L CTMAB2.5, 1.63 g/L TiO_2, pH at 3.5 and time for 60 min. Thus aeration was not a major portion of removal

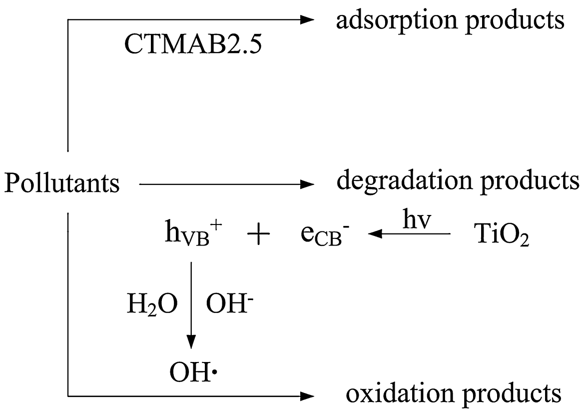

Fig. 7. The reaction scheme of pollutants, CTMAB2.5 and TiO_2.

mechanism and was maintained at 0.4 L/min to keep CTMAB2.5 and TiO_2 suspending.

In spite of being powerful oxidation, photocatalysis could be detrimentally influenced by HCO_3^- due to scavenging of oxidizing holes and radicals [7]. HCO_3^- concentration of leachate was nearly 0.08 mol/L measured by pH indicator titration. So the interference of HCO_3^- on photocatalytic degradation was less prominent.

Taking great removal into account, pretreating technology of combination CTMAB2.5 adsorption and TiO_2 photocatalysis was feasible. Kurniawan and Lo [33] researched similar treatment integrateing advanced oxidation process and adsorption which achieved COD removal of 82% and NH_3-N removal of 59% under the condition of 1:5 (H_2O_2:GAC) dose ratio and pH 8.0.

3.4. RSM experimental data analysis

Response variables of COD and NH_3-N removal were acquired from 30 groups of experiments that were summarized in Table 3.

3.4.1. Data analysis of COD removal as the response variable

The relationship between COD removal (y_1) and four operating variables (x_1–x_4) was represented in the form of following polynomial Eq. (3):

$$\begin{aligned} y_1 = {} & 49.83 + 4.04x_1 + 1.04x_2 - 5.13x_3 - 0.38x_4 - 7.06x_1x_2 \\ & - 6.06x_1x_3 + 0.063x_1x_4 + 3.06x_2x_3 + 2.19x_2x_4 + 1.44x_3x_4 \\ & - 1.59x_1{}^2 - 0.97x_2{}^2 + 7.03x_3{}^2 - 0.22x_4{}^2 \end{aligned} \quad (3)$$

Statistical testing of this model was carried out by Fisher's statistical method for analysis of variance (ANOVA) [27]. Results were shown in Table 4 and implied that second-order equation fitted well because model *F*-value of 8.47 was greater than $F_{0.01}(14, 15) = 3.56$, value of Prob > *F* < 0.0001 was less than 0.05, and total determination coefficient R^2 reached 0.8877.

Fig. 8(a) clearly showed COD removal with the variation of CTMAB2.5 dosage and pH and the interaction between CTMAB2.5 and pH mutually influenced COD removal. With CTMAB2.5 dosage at low levels, COD removal was higher with the advance of pH. When CTMAB2.5 dose was low, photocatalytic oxidation played main role in degrading COD. The initial step was mainly direct hole oxidation. While pH increased, it shifted progressively to a hydroxyl radical-like reaction following rate-limiting hole oxidation of surface hydroxyls [34]. Cho et al. [34] also reported similar phenomenon that especially at pH 4.0, degradation rate was distinctly higher than at pH 2.0. However, with CTMAB2.5 dosage at high levels, the higher removal of COD was obtained at lower pH. When CTMAB2.5 dose was high, its adsorption performance was superior in removing pollutant. In acid conditions, CTMAB2.5 was strongly favored to adsorb pollutants and TiO_2 was also favored to generate electron–hole pair and hydroxylation of TiO_2 surface. The latter result could accelerate the formation of OH• and the occurrence of photoxidation. Inversely, in alkaline environment, there is a Coulombic repulsion between the negative charged surface of photocatalyst and the hydroxide anions [21]. This fact could prevent the formation of OH· and thus decrease the photoxidation. Besides, in alkaline environment, not only the effective aperture of CTMAB2.5 could shrink to influence the adsorption, but also organic matters were in stable non-dissociation state and hard to be removed.

The greatest COD removal arrived at 89% with CTMAB2.5 dosage of 5.0 g/L, pH at 5.0, TiO_2 dosage of 0.5 g/L and reaction time for 90 min in 30 sets experiments.

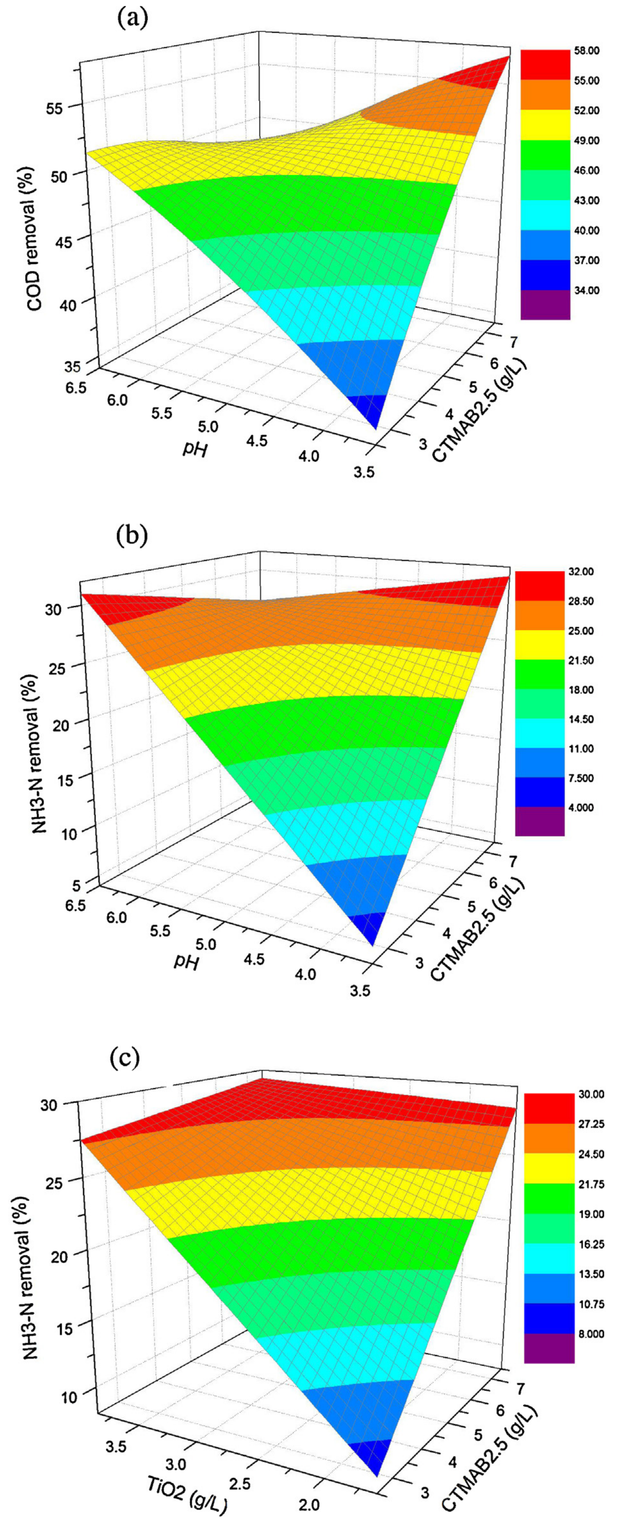

Fig. 8. Surface graphs of COD and NH_3-N removal efficiency showing the effect of variables: (a) and (b) CTMAB2.5–pH with TiO_2 dosage = 2.75 g/L and reaction time = 90 min, (c) TiO_2–CTMAB2.5 with reaction time = 90 min and pH = 5.0, respectively.

Table 4
ANOVA for COD removal analysis of variance and adequacy of the quadratic model.

Source	Sum of squares	Degrees of freedom	Mean square	*F*-value	Prob > *F*
Model	4334.78	14	309.63	8.47	<0.0001
x_1	392.04	1	392.04	10.72	0.0051
x_3	630.38	1	630.38	17.24	0.0009
x_1x_2	798.06	1	798.06	21.82	0.0003
x_1x_3	588.06	1	588.06	16.08	0.0011
x_3^2	1356.03	1	1356.03	37.08	<0.0001
Residual	548.58	15	36.57		
Lack of fit	527.75	10	52.78	12.67	0.0059
Pure error	20.83	5	4.17		

S.D. = 6.05, PRESS = 3069.84, $R^2 = 0.8877$, Adj. $R^2 = 0.7828$, Adeq precision = 12.355.

3.4.2. Data analysis of NH_3-N removal as the response variable

Final equation in terms of code factors between the NH_3-N removal (y_2) and four operating variables (x_1–x_4) was represented in the form of following polynomial Eq. (4):

$$y_2 = 23.57 + 5.33x_1 + 5.25x_2 + 4.83x_3 - 0.083x_4 - 7.50x_1x_2 - 4.38x_1x_3 + 0.88x_1x_4 + 10.00x_2x_3 - 1.75x_2x_4 - 0.087x_3x_4 \quad (4)$$

Results of ANOVA were listed in Table 5 and implied that second-order equation fitted well, because model *F*-value of 8.32 was greater than $F_{0.01}(10, 19) = 3.43$, value of 'Prob > *F*' < 0.0001 was less than 0.05, and total determination coefficient R^2 achieved 0.8141.

Fig. 8(b) showed NH_3-N removal with the variation of CTMAB2.5 dosage and pH. NH_3-N removal predominantly elevated with the advance of CTMAB2.5 dosage due to the adsorption. The decomposition of NH_3-N at higher pH was significantly greater than at lower pH. The results agreed with similar reports [25,34] and the reasons could be as follows. Firstly, the amounts of hydrogen ion were large at low pH in water. Hydrogen ions with smaller radius were easier to be adsorbed by organobentonite than ammonia ions with larger radius. Secondly, the concentration of OH^- was enhanced with the advance of pH. It availed to generate $OH^\bullet$ and enhance the attraction between the ammonium ions and catalyst surface to promote photocatalysis reaction [23]. Thirdly, at high pH, the proportion of ammonia in the form of $NH_3{\cdot}H_2O$ which could be stripped was improved. According to the experiment of capping or not on the reactor, nearly 2% NH_3-N was stripped out of solution.

Fig. 8(c) displayed NH_3-N removal with variation dosages of CTMAB2.5 and TiO_2. The sharp curvatures showed that the response of NH_3-N removal was greatly sensitive to two process variables. TiO_2 dosage was an important factor because it impacted on the amount of producing $OH^\bullet$ which directly determined the ability of photocatalysis. Theoretically, the more TiO_2 dosage was, the better removal was obtained. However, TiO_2 dosage should be appropriate. Because few dosages could not convey effective photons to chemical energy, while excessive dosages were easy to produce turbid solution, cause light scattering and reduce the adsorption rate of ultraviolet light.

The maximum removal of NH_3-N was 61% in 30 sets of experiments with CTMAB2.5 dosage of 2.5 g/L, pH at 6.5, TiO_2 dosage of 3.88 g/L, and reaction time for 60 min.

3.5. The contrastive analysis of removal of COD and NH_3-N

According to RSM, optimal operation condition calculated from the regression equations was CTMAB2.5 dosage of 7.5 g/L, pH at 3.5, TiO_2 dosage of 1.63 g/L, and reaction time for 60.02 min, which maintained removal of COD and NH_3-N at 82% and 37%. In general, average removal efficiency of ammonia was only half of the organic matters in 30 experiments. Primarily, ammonia removal was pH-dependent, especially under alkaline conditions. However, from the angle of removing organic compounds, the reactor was mostly set in acid condition, which limited ammonia removal artificially. Secondly, it was hypothesized that the presence of intricate constituents in the leachate had implications on ammonia removal. They competed with ammonia for reaction sites. And ammonia was in a competitive disadvantage due to its characteristic. Other paper also reported the phenomenon [24] that ammonia removal of practical leachate including complex constituents was much lower than ammonia removal of simulated leachate only containing ammonia pollutant.

3.6. Analysis of effluent quality

After the treatment under optimal reaction condition, the average value of BOD_5 measured by dilution and seeding method [35] was 315 mg/L ranging from 290 to 350 mg/L. This brought good result that the biodegradability of leachate was improved, with an increase in BOD_5/COD ration from 0.11 to 0.32. However, the treated effluent could not comply with COD limit of lower than 100 mg/L and NH_3-N discharge standard of less than 25 mg/L. Therefore, further treatments such as biological treatment or membrane filtration technology to complement the degradation of leachate are still required to meet local regulation.

Table 5
ANOVA for NH_3-N removal analysis of variance and adequacy of the quadratic model.

Source	Sum of squares	Degrees of freedom	Mean square	*F*-value	Prob > *F*
Model	4784.75	10	478.48	8.32	<0.0001
x_1	682.67	1	682.67	11.87	0.0027
x_2	661.50	1	661.50	11.50	0.0031
x_3	560.67	1	560.67	9.75	0.0056
x_1x_2	900.00	1	900.00	15.65	0.0008
x_1x_3	306.25	1	306.25	5.33	0.0324
x_2x_3	1600.00	1	1600.00	27.82	<0.0001
Residual	1092.62	19	57.51		
Lack of fit	1072.62	14	76.62	19.15	0.0021
Pure error	20.00	5	4.00		

S.D. = 7.58, PRESS = 3462.62, $R^2 = 0.8141$, Adj. $R^2 = 0.7163$, Adeq precision = 10.707.

4. Conclusions

Through the representation of CTMAB2.5 by FESME/EDS and FTIRS, we confirmed that $CTMA^+$ were successfully loaded on the surface of bentonite and greatly enhanced its performance of adsorption.

The combination of CTMAB2.5 and TiO_2 was superior to either running alone. Furthermore, removal efficiency of simultaneously utilizing CTMAB2.5 and TiO_2 was better than them in succession. So pretreating technology of combination was feasible.

In practical experiments, at different conditions, maximum removal of COD and NH_3-N reached 89% and 61%, respectively. According to RSM, the optimal operation conditions calculated from the regression equations were CTMAB2.5 dosage at 7.5 g/L, pH at 3.5, TiO_2 dosage at 1.63 g/L, and reaction time for 60.02 min, which maintained removal of COD and NH_3-N at 82% and 37%. The values of COD and NH_3-N removal in verification experiment operated under the optimal condition arrived at 86% and 41%, respectively.

Acknowledgment

This project was supported by the National Natural Science Foundation of China (51378189 and 51078131).

References

[1] J. Labanowski, V. Pallier, G.F. Cathalifaud, Study of organic matter during coagulation and electrocoagulation processes: application to a stabilized landfill leachate, J. Hazard. Mater. 179 (2010) 166–172.

[2] T.A. Kurniawan, W.H. Lo, G.Y.S. Chan, Physico-chemical treatment for removal of recalcitrant contaminants from landfill leachate, J. Hazard. Mater. B129 (2006) 80–100.

[3] X.Z. Li, Q.L. Zhao, MAP precipitation from landfill leachate and seawater bitter waste, Environ. Technol. 23 (2002) 989–1000.

[4] R.H. Kettunen, J.A. Rintala, Performance of an on-site UASB reactor treating leachate at low temperature, Water Res. 32 (3) (1998) 537–546.

[5] B.U. Bae, E.S. Jung, Y.R. Kim, H.S. Shin, Treatment of landfill leachate using activated sludge process and electron-beam radiation, Water Res. 33 (11) (1999) 2669–2673.

[6] S. Ghafari, H.A. Aziz, M.H. Isa, A.A. Zinatizadeh, Application of response surface methodology (RSM) to optimize coagulation–flocculation treatment of leachate using poly-aluminum chloride (PAC) and alum, J. Hazard. Mater. 163 (2009) 650–656.

[7] T.A. Kurniawan, W.H. Lo, G.Y.S. Chan, Radicals-catalyzed oxidation reactions for degradation of recalcitrant compounds from landfill leachate, Chem. Eng. J. 125 (2006) 35–57.

[8] T.A. Kurniawan, W.H. Lo, G.Y.S. Chan, Degradation of recalcitrant compounds from stabilized landfill leachate using a combination of ozone-GAC adsorption treatment, J. Hazard. Mater. B 137 (2006) 443–455.

[9] Z.P. Wang, Z. Zhang, Y.J. Lin, N.S. Deng, T. Tao, K. Zhuo, Landfill leachate treatment by a coagulation–photooxidation process, J. Hazard. Mater. B 95 (2002) 153–159.

[10] N. Schwarzenbeck, K. Leonhard, P.A. Wilderer, Treatment of landfill leachate-high tech or low tech, Water Sci. Technol. 48 (2003) 277–284.

[11] L.D. Palma, P. Ferrantelli, C. Merli, E. Petrucci, Treatment of industrial landfill leachate by means of evaporation and reverse osmosis, Waste Manage. 22 (2002) 951–955.

[12] L.Z. Zhu, Y.M. Li, J.Y. Zhang, Sorption of organobentonites to same organic pollutants in water, Environ. Sci. Technol. 31 (1997) 1407–1410.

[13] Y.H. Shen, Removal of phenol from water by adsorption–flocculation using organobentonite, Water Res. 36 (2002) 1107–1114.

[14] L.Z. Zhu, X.G. Ren, S.B. Yu, Use of cetyltrimethylammonium bromide–bentonite to remove organic contaminants of varying polar character from water, Environ. Sci. Technol. 32 (1998) 3374–3378.

[15] J.A. Smith, P.R. Jaffe, C.T. Chiou, Effect of ten quaternary ammonium cations on tetrachloromethane sorption to clay from water, Environ. Sci. Technol. 24 (1990) 1167–1172.

[16] P. Baskaralingam, M. Pulikesi, D. Elango, V. Ramamurthi, S. Sivanesan, Adsorption of acid dye onto organobentonite, J. Hazard. Mater. B 128 (2006) 138–144.

[17] J. Wanger, H. Chen, B.J. Brownawell, J.C. Westall, Use of cationic surfactants to modify soil surfaces to promote sorption and migration of hydrophobic organic compounds, Environ. Sci. Technol. 28 (1994) 231–237.

[18] L.Z. Zhu, B.L. Chen, S. Tao, C.T. Chiou, Interactions of organic contaminants with mineral-adsorbed surfactants, Environ. Sci. Technol. 37 (2003) 4001–4006.

[19] B.L. Chen, W.H. Huang, J.F. Mao, S.F. Lv, Enhanced sorption of naphthalene and nitroaromatic compounds to bentonite by potassium and cetyltrimethylammonium cations, J. Hazard. Mater. 158 (2008) 116–123.

[20] H. Ling, A.H. Lu, C.Q. Wang, Y. Li, P. Chen, J. Wang, J. Zhou, Treatment of municipal landfill leachate with organically modified bentonite, Clays Clay Miner. 59 (2011) 518–524.

[21] U.G. Akpan, B.H. Hameed, Parameters affecting the photocatalytic degradation of dyes using TiO_2-based photocatalysts: a review, J. Hazard. Mater. 170 (2009) 520–529.

[22] R. Poblete, E. Otal, L.F. Vilches, J. Vale, C. Fernandez-Pereira, Photocatalytic degradation of humic acid and landfill leachate using a solid industrial by product containing TiO_2 and Fe, Appl. Catal. B: Environ. 102 (2012) 172–179.

[23] Y. Shavisi, S. Sharifnia, S.N. Hosseini, M.A. Khadivi, Application of TiO_2/perlite photocatalysis for degradation of ammonia in wastewater, J. Ind. Eng. Chem. 20 (2014) 278–283.

[24] W.Y. Wang, A. Irawan, Y. Ku, Photocatalytic degradation of Acid Red 4 using a titanium dioxide membrane supported on a porous ceramic tube, Water Res. 42 (2008) 4725–4732.

[25] D.E. Meeroff, F. Bloetscher, D.V. Reddy, F. Gasnier, S. Jain, A. McBarnette, H. Hamaguchi, Application of photochemical technologies for treatment of landfill leachate, J. Hazard. Mater. 209–210 (2012) 299–307.

[26] M. Otto, Chemometrics, Wiley-VCH Verlag, Weinheim, 1998.

[27] J. Huang, Z.H. Yang, G.M. Zeng, M. Ruan, H.Y. Xu, Influence of composite flocculant of PAC and MBFGA1 on residual aluminum species distribution, Chem. Eng. J. 191 (2012) 269–277.

[28] Water quality – Determination of the chemical oxygen demand – Dichromate method GB 11914-89.

[29] Water quality – Determination of ammonia nitrogen – Nessler's reagent spectrophotometry HJ 535-2009.

[30] B.J. Hu, H.J. Luo, Adsorption of hexavalent chromium onto montmorillonite modified with hydroxyaluminum and cetyltrimethylammonium bromide, Appl. Surf. Sci. 257 (2010) 769–775.

[31] S.Q. Liu, H. Li, W.H. Sun, X.M. Wang, Z.G. Chen, J.J. Xu, H.X. Ju, H.Y. Chen, Photoinducedly electrochemical preparation of Prussian blue film and electrochemical modification of the film with cetyltrimethylammonium cation, Electrochim. Acta 56 (2011) 4007–4014.

[32] D. Hao, Z.M. Yang, C.H. Jiang, J.S. Zhang, Synergistic photocatalytic effect of TiO_2 coatings and p-type semiconductive SiC foam supports for degradation of organic contaminant, Appl. Catal. B: Environ. 144 (2014) 196–202.

[33] T.A. Kurniawan, W.H. Lo, Removal of refractory compounds from landfill leachate using an integrated H_2O_2 oxidation and granular activated carbon (GAC) adsorption treatment, Water Res. 43 (2009) 4079–4091.

[34] S.P. Cho, S.C. Hong, S. Hong, Photocatalytic degradation of the landfill leachate containing refractory matters and nitrogen compounds, Appl. Catal. B: Environ. 39 (2002) 125–133.

[35] Water quality – Determination of biochemical oxygen demand after 5 days (BOD5) for dilution and seeding method HJ 505-2009.